ELSEVIER

Biochimica et Biophysica Acta 1512 (2001) 291–298

BIOCHIMICA ET BIOPHYSICA ACTA
BBA

www.bba-direct.com

The structure of the HIV-1 Vpu ion channel: modelling and simulation studies

F.S. Cordes [a], A. Kukol [1,b], L.R. Forrest [a], I.T. Arkin [2,b], M.S.P. Sansom [a], W.B. Fischer [a,*]

[a] *Laboratory of Molecular Biophysics, Department of Biochemistry, Oxford University, South Parks Road, Oxford OX1 3QU, UK*
[b] *Cambridge Centre for Molecular Recognition, Department of Biochemistry, University of Cambridge, Cambridge CB2 1GA, UK*

Received 1 February 2001; received in revised form 5 April 2001; accepted 6 April 2001

Abstract

Vpu is an 81 amino acid auxiliary protein in HIV-1 which exhibits channel activity. We used two homo-pentameric bundles with the helical transmembrane segments derived from FTIR spectroscopy in combination with a global molecular dynamics search protocol: (i) tryptophans (W) pointing into the pore, and (ii) W facing the lipids. Two equivalent bundles have been generated using a simulated annealing via a restrained molecular dynamics simulations (SA/MD) protocol. A fifth model was generated via SA/MD with all serines facing the pore. The latter model adopts a very stable structure during the 2 ns of simulation. The stability of the models with W facing the pore depends on the starting structure. A possible gating mechanism is outlined.

Keywords: HIV-1; Vpu; Viral ion channel; Molecular dynamics; Gating

1. Introduction

The genome of the enveloped virus HIV-1 encodes a small auxiliary phosphoprotein with a length of 81 amino acids called Vpu [1,2]. It is composed of a hydrophobic transmembrane (TM) domain (amino acids 1–27, N-terminal end) and a hydrophilic cytoplasmic domain of 54 amino acids (C-terminal end) [3]. Vpu is not found in the envelope of the virus particle but is expressed to the membranes of subcellular compartments of the infected cell [4]. Vpu has two major roles in the life cycle of the virus: (i) it controls the release/secretion of virus particles from the cell surface [5,6], and (ii) it mediates the degradation of the CD4 protein in the endoplasmic reticulum (ER) [7,8]. The TM segment of Vpu is responsible for particle release/secretion [9] whereas the cytoplasmic site is essential for degradation of CD4 protein [8–10].

There is reasonable, if not conclusive, evidence that Vpu can form ion channels: Vpu expressed in *Escherichia coli*, purified and reconstituted in planar lipid bilayer shows channel activity [11], also a synthetic peptide corresponding to the putative TM segment of Vpu exhibits channel activity [12,13]. However, final proof of channel activity with a channel blocking agent is still lacking.

* Corresponding author. Fax: +44-1865-27-52-34; E-mail: wolfgang@bioch.ox.ac.uk
[1] Present address: Department of Biological Science, University of Warwick, Coventry CV4 7AL, UK.
[2] Present address: Institute of Life Science, Department of Biological Chemistry, Hebrew University, Jerusalem, Israel.

0005-2736/01/$ – see front matter
PII: S0005-2736(01)00332-7

NMR [13–17], CD [18], and FTIR spectroscopic data [19,20] of the synthesized putative TM segments of several channel peptides reveal a high helical content of the peptides reconstituted in lipid bilayers. Also various secondary structure prediction methods predict a single helical segment for all the viral ion channel peptides which is consequently assumed to span the bilayer [21]. Self-assembly is a characteristic feature of Vpu in vivo as well as in vitro [3,22]. The exact number of homo-oligomers which form the channel is not yet known. Molecular modelling simulation studies suggest the formation of at least five parallel helices to form an ion channel [23,24].

In recent experiments FTIR spectroscopy was used to elucidate the orientation of the putative TM segment of Vpu (AIV A^{10} LVVAIIIAI V^{20} VWSIVIIE) [19] in a lipid bilayer. Thereby specific isotopic labelled (^{13}C) amino acids were incorporated in the TM segment. In combination with a global molecular dynamics (MD) search protocol the following structural model is proposed [19]: a bundle consisting of five identical segments (homo-pentamer) with the tryptophan in each of the segments pointing into the pore. We use this structure and perform a 2 ns molecular modelling simulation in a fully hydrated bilayer. We also investigate a bundle with all tryptophans facing the lipid phase from the same study [19]. In comparison two similar structures, with respect to the orientation of the tryptophans, are built using a simulated annealing via restrained molecular dynamics simulations (SA/MD) protocol [25,26]. An additional structure is created by SA/MD with the serine residues pointing into the pore. With this study we aim to assess which of the bundles seems to be an energetically stable structure.

2. Materials and methods:

2.1. Modelling

Bundles of Vpu segments derived from Arkin and co-workers [19] are based on a FTIR spectroscopic analysis on the orientation of the putative TM segment of Vpu (22 amino acids: AIV A^{10} LVVAIIIAI V^{20} VWSIVIIE) reconstituted into vesicles. The analysis of the spectroscopic data leads to a helix tilt angle (angle between membrane normal and helix axis) of 6° and pitch angles (angle between two consecutive residues in an α-helix; $\omega_{i+1} = 100°$ for a standard α-helix) of $\omega_{i+7} = (283 \pm 11)°$ for the ^{13}C labels Val^{13}/Val^{20} and $\omega_{i+7} = (23 \pm 11)°$ for the ^{13}C labels Ala^{14}/Val^{21}. A global MD search protocol without any restraints on homo-tetra-, penta- and hexameric bundles releases a set of 288 structures. A detailed description of the data generation is given elsewhere [19,27]. In brief, calculations are done with idealized helices (rise/residue = 1.5 Å; 3.6 residues per turn) in vacuo. Symmetric tetramers, pentamers and hexamers ($n = 4, 5, 6$) are generated by replicating the helix and rotating it by $360°/n$ around the centre of the bundle. An initial crossing angle of 25° for left-handed and −25° for right-handed bundle is applied by rotating the long helix axis with respect to the long bundle axis. Rotations simultaneously to all helices are carried out between 0° and 360° in steps of 10°. Using different initial random atom velocities four trials with each starting structure are carried out. This results in $36 \times 4 \times 2 = 288$ structures. For each structure a simulated annealing and energy minimization protocol is applied. Structures are clustered (minimum of 10 structures) if the root mean square deviation (RMSD) is ≤0.1 nm. For each cluster an average structure is calculated, energy minimized and used in the same simulated annealing protocol as mentioned above.

The model with the pitch angle ($\omega_{i+7} = 316°$ (Val^{13}) and 55° (Ala^{14})) closest to the experimental values ($\omega_{i+7} = 283° \pm 11°$ and $23° \pm 11°$; helix tilt $\beta = 6.5° \pm 11°$), a homo-pentamer, is one of the energetically most favourable bundles (W-in) (Table 1). The second pentameric model is chosen so that all tryptophans point towards the lipid phase (W-out).

We also generate three pentameric models using a SA/MD protocol [25,26] based on the programme Xplor [28], implementing a starting tilt angle of 5°. The SA/MD protocol comprises two stages: in stage 1 bundles of n (number of segments, here $n = 5$) parallel, idealized α-helices are constructed corresponding to the Cα atoms of the peptide unit. All other atoms of the individual amino acids are superimposed. During stage 1 these other atoms 'evolve' from the Cα atoms remaining fixed. Beginning the annealing at 1000 K weights for bond length, bond angles, planarity and chirality are gradually increased. A repulsive van der Waals term is slowly

introduced after an initial delay. After reaching the final scaling factors of these components of the empirical energy function the bundle is cooled to 300 K, in steps of 10 K per 0.5 ps. Van der Waals radii are reduced to 80% during this stage. This allows the atoms to pass each other. We obtain five structures for each bundle. Each structure from stage 1 will be used for five molecular dynamics runs in stage 2. In stage 2 initial velocities correspond to 500 K. Harmonic restraints hold the Cα atoms, but are relaxed as the temperature drops from 500 to 300 K. At this stage distance restraints are also introduced. At 300 K a constant temperature dynamics for 5 ps is performed, followed by a 1000 steps of conjugate gradient energy minimization. Now, also the Cα atoms are allowed to move. In stage 2 electrostatic interactions are introduced into the potential energy function. The main chain atoms obtain their charges corresponding to the PARAM19 parameter set. Partial charges on side chain atoms of polar side chains are gradually scaled up (from 0.05 to 0.4 times their full value) during the temperature reduction from 500 to 300 K. The scaling factor 0.4 is also applied during the 5 ps dynamics and energy minimization. A distance dependent dielectric function is used, with a switching function smoothly truncating distant electrostatic interactions. In stage 2 we obtain $5 \times 5 = 25$ structures. The most symmetric structure in respect to the pseudo 5-fold symmetry axis of the bundle is chosen for the simulations.

Two of the models (W^X-in and W^X-out) are equivalent to W-in and W-out in respect to the orientation of the tryptophans: W^X-in (tryptophans point into the pore, generated by XPLOR 'W^X') and W^X-out (tryptophans point towards the pore). A third 'best guess' model is built using Xplor with all serines facing the pore (S^X-in, starting tilt angle 5°). The rationale for a bundle like this is based on the findings in other ion channels: (i) hydrophilic residues, such as serines, line the pore of the channel (e.g. like in nicotinic acetylcholine receptor derived from mutagenesis data [29–32]), and (ii) tryptophans are located at a hydrophobic/hydrophilic interface (e.g. porin [33], bacteriorhodopsin [34]).

2.2. Simulations and analysis

All five of the helix bundles were placed in holes (approx. 6×6 nm^2) within a lipid bilayer of 1-palmitoyl-2-oleoyl-*sn*-glycerol-3-phosphatidylcholine (POPC) and consequently solvated with more than 30 water molecules (SPC water model [35]) per lipid, resulting in a system of approx. 20 000 atoms [21]. Simulations were run for 2 ns using GROMACS 1.6 software (http://rugmd0.chem.rug.nl/~gmx/gmx.html) on a 10 processor SGI Origin 2000 machine. For data analysis Gromacs and DSSP [36] software was used. The structures were visualized with the programme MOLSCRIPT. To assess whether a structure has reached equilibrium, the RMSD of the Cα atoms (peptide unit) are consecutively related to structures at selected time steps, i.e. 1000 ps, 1500 ps, and 2000 ps using the protocol in [37].

3. Results

In Fig. 1 the RMSD values of all five structures are presented. A step descent or ascent of the values to or from the reference value indicates a non-equilibrated system. W-in is not yet equilibrated during the 2 ns simulation (Fig. 1A). W^X-in (Fig. 1B) seems to adopt an equilibrated structure: a descending curve at the beginning of the simulation reaching a plateau without any major descent and ascent around the reference points. The RMSD values for the bundle W-out (Fig. 1C) and to a slightly lesser extend for W^X-out (Fig. 1D) both reach a similar plateau after the first half of the simulation. The values for the 'best guess' model S^X-in (Fig. 1E) level off after approx. 400 ps.

Table 1
Pentameric bundles of Vpu (AIV A^{10} LVVAIIIAI V^{20} VWSIVIIE) used in this study

W-in	Structure derived from Kukol et al. [19] by FTIR spectroscopy: all tryptophans facing the pore
W^X-in	Structure generated using Xplor: tryptophans facing the pore
W-out	Structure derived from Kukol et al. [19] by FTIR spectroscopy: all tryptophans pointing towards the lipid phase
W^X-out	Structure generated using Xplor: tryptophans pointing towards the lipid phase
S^X-in	'Best guess' model, generated using Xplor: serines facing the pore, tryptophans are located at the peptide/lipid/lipid-head-group interface

3.1. Structure of the bundles

A view down the pore from the N terminus to the C terminus of W-in and S^X-in at 0 ns and 2 ns simulation is shown in Fig. 2. In W-in the tryptophans completely block the pore of the bundle in the starting structure (Fig. 2A), with the serines facing the hydrophobic segment of the bilayer. At the end of the simulation the situation has drastically changed: two segments seem to escape from the assembly, one segment with its C-terminal end, the other with its N-terminal end. S^X-in forms a bundle with a slightly left-handed super coiling (Fig. 2B). After 2 ns of simulation this coiling is still visible and the tryptophans are located at the helix-helix/helix-lipid interface. In addition, the serines have moved closer to their adjacent helices. Fig. 3 shows W-out, W^X-out, and W^X-in after 2 ns of simulation. For W^X-in all tryptophans remain facing the pore at the end of the simulation.

For all bundles the tilt angle converges towards a mean value of 15° (W-in: 16° ± 4°, W^X-in: 14° ± 4°, W-out: 11° ± 4°, W^X-out: 11° ± 4°, S^X-in: 13° ± 5°). These values are in the same order of those values found for bundles of Vpu in a low dielectric slab mimicking a lipid bilayer [38]. The averaged inter-helix crossing angle (angle with which two adjacent helices cross each other) does not show any trend for the models under investigation (W-in: 11° ± 7°, W^X-in: 14° ± 6°, W-out: 14° ± 9°, W^X-out: 8° ± 4°, S^X-in: 15° ± 9°). Also the average inter-helix distance remains around 1.1–1.2 nm for all bundles.

3.2. Hydrogen bonding

We analysed the fraction of hydrogen bonding f_H ($f_H = n_H/n_T \cdot q$), where n_H is the total number of time steps during which the residues form hydrogen bonds, n_T the total number of time steps in the simulation, and q the number of observed hydrogen bonds formed by the residue) of the serines and tryptophans. The fraction of each residue in the individual segments of the bundles is shown in parentheses

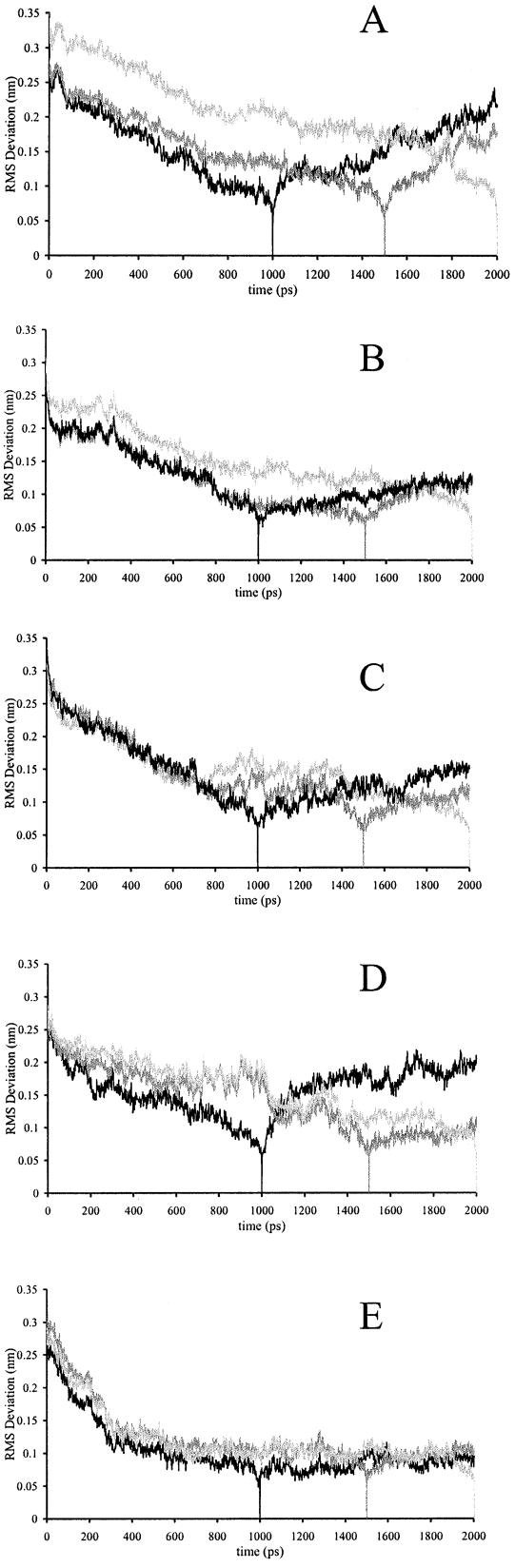

→

Fig. 1. Cα RMSD versus time calculated for reference conformations at 1000 (black), 1500 (grey), and 2000 ps (light). (A) W-in; (B) W^X-in; (C) W-out; (D) W^X-out; (E) S^X-in.

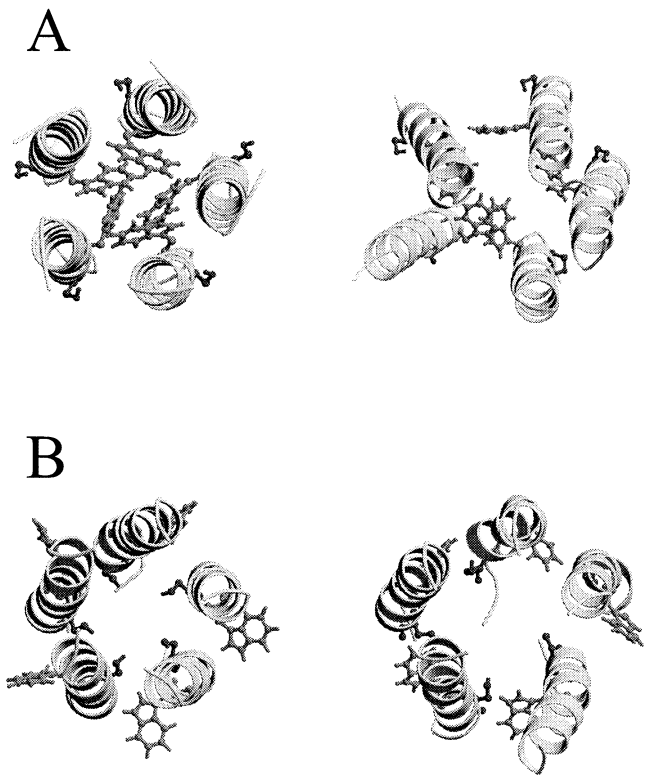

Fig. 2. Top view of the bundles. (A) W-in; (B) S^X-in. In both panels at 0 ns (left) and 2 ns (right). Tryptophans and serines are drawn in stick and ball modus. Figures are generated with MOLSCRIPT.

(see below). An explanation of the hydrogen bonding analysis is given in more detail elsewhere [21,39]. High values of f_H indicate that the residues remain hydrogen bonded with only a few partners over the entire simulation, low values indicating that the residue is either involved in hydrogen bonding for a short fraction of the time or that there is a high number of changing partners for hydrogen bonding.

Some of the tryptophans in W-in form hydrogen bonds with neighbouring segments (f_H: 0.13, 0.03, 0.06). Since the tryptophans are in the pore they also undergo hydrogen bonding with pore waters (f_H: 0.03, 0.02, 0.02, 0.03). All serines show hydrogen bonding preferentially with carbonyl functionality of the peptide unit (backbone) within their own segment (f_H: 0.26, 0.27, 0.18, 0.37, 0.22). Only one serine forms hydrogen bonds with water molecules (f_H: 0.07). A similar pattern is derived with the bundle W^X-in (data not shown).

For two tryptophans in S^X-in hydrogen bonding with the backbone of their neighbours is observed (f_H: 0.22, 0.07). The serines show preferential hydrogen bonding with the backbone of the same segment (f_H: 0.15, 0.10, 0.05, 0.07, 0.39). One serine does show hydrogen bonding with a side chain of a neighbouring segment (f_H: 0.21). In addition, nearly all of the serines form hydrogen bonds to water molecules (f_H: 0.04, 0.04, 0.03, 0.03).

The tryptophans in W-out and W^X-out lack any major hydrogen bonding (data not shown). The serines in both of these bundles interact either with the backbone of their own segment or with a neighbouring segment, although interactions with water molecules are also found.

4. Discussion

Without any structure for the short TM spanning viral peptides, it still remains an intriguing task as to how the individual segments are orientated to form a proper ion conducting pore [40]. A common scheme is to orient the hydrophilic residues within a hydrophobic TM segment in such a way that all these

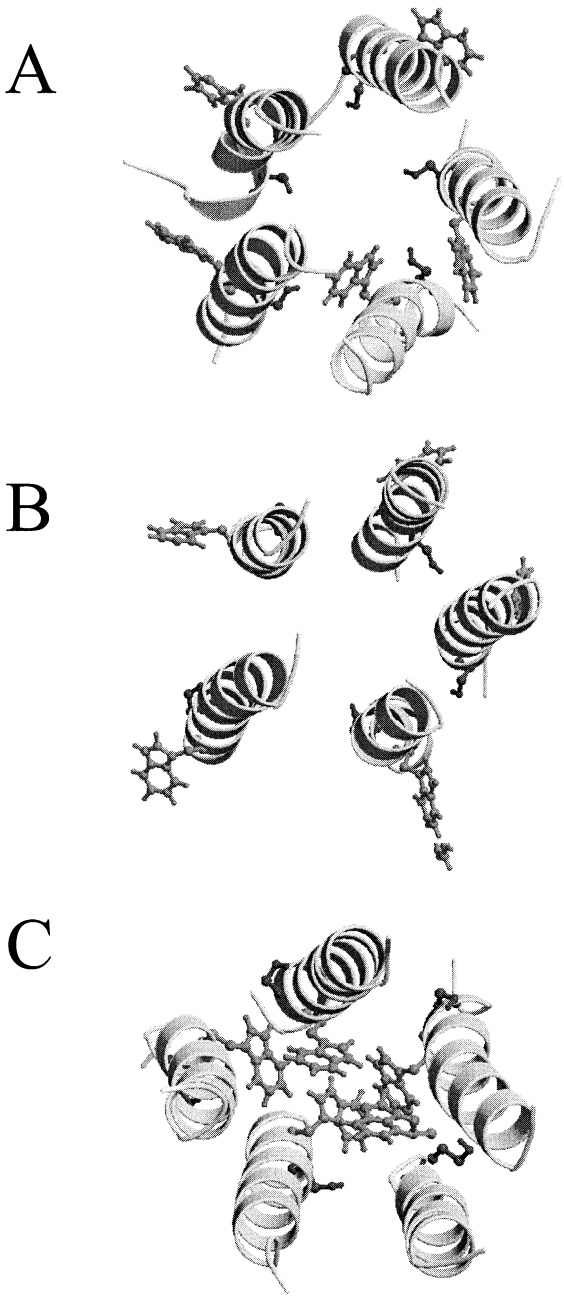

Fig. 3. Model of W-out (A), W^X-out (B), and W^X-in (C) after 2 ns of simulation (top view). Tryptophans and serines are indicated as in Fig. 2. Lipids and water molecules omitted for clarity.

residues point towards the centre of the bundle. This would consequently restrain the position of other residues, e.g. the tryptophans. In such an orientation (serines facing the pore in this study) the tryptophans are most likely located at the helix-helix and helix-lipid head group interface. Orientation of tryptophans at the helix-lipid head group interface is also experimentally confirmed for other ion channel peptides such as gramicidin [41–44]. Tryptophans and phenylalanines of the channel pore porin are also located at the outer side of the protein aligned towards the lipid head groups [45]. Model S^X-in satisfies the intention about the alignment to form ion conducting pores of peptides or proteins. This model places the tryptophans towards the helix-helix/helix-lipid head group interface. The computational simulations reveal that this model adopts the most stable structure during the 2 ns simulation.

For bacteriorhodopsin tryptophans are also found within the interior of the protein. Some of them are essential to support proton translocation (see examples in [46–48]). In the case of M2 from influenza A, alignment of Ser-31 and His-37 towards the centre of the bundle automatically orients Trp-41 into the same direction [49]. These tryptophans would also occlude the pore; however, tetrameric bundles of M2 are characterized by a large tilt or tepee-like structure in the simulations, thereby having a wider opening towards the C terminus [50–52]. Solid state NMR revealed tilt angles ($>30°$ [53,54]) which are larger than for Vpu ($<30°$ [55–57]). It seems likely that the tryptophans contribute to the overall structure of the TM segments of influenza's M2. Thus, the Vpu model proposed by Kukol and Arkin [19] would not be unique in respect of its tryptophan orientation. Serines and tryptophans are the only residues capable of forming hydrogen bonds within the otherwise highly hydrophobic TM segment of Vpu. This motif (long hydrophobic segment with two adjacent hydrophilic residues towards the C-terminal end) is probably one of the reasons for Vpu's conductance of ions and insensitivity to amantadine as outlined in [55].

A global molecular dynamics search protocol on tetrameric, pentameric and hexameric bundles has been used to generate clusters of possible structures of such bundles [19]. Bundle structure W-in corresponds to one cluster for which the structure coincides reasonably with experimental data from FTIR spectroscopy regarding only the pitch angle ω. However, the very low tilt angle from the experiment ($6.5 \pm 1.7°$ [19]) limits the possibility to obtain proper pitch angles with spectroscopic methods (solid state

NMR: $< 30°$ [55–57]) as discussed in [19]. Nevertheless, the low energy of W-in ($E = -182$ kcal/mol) from the global search analysis in the absence of water during the calculations makes this bundle a possible model for an energetically stable structure.

Simulations of W-in on a longer time scale and in fully solvated lipid bilayer suggest that the segments rotate away from each other forcing the tryptophans between the helices and closer to the lipid head group region. During the in vacuo simulations [19], the tryptophans might be held together by inter-hydrogen bonding. The result is the 'low energy' structure W-in. In the present simulation the water molecules might compete for hydrogen bonding and consequently weaken the hydrogen bonding between the tryptophan residues. As a consequence the segments are able to drift apart because of repulsive forces. However, during the simulations of W^X-in no 'opening' of the channel is observed. Thus, the highly occluded pore does not necessarily repel the segments or induce a rotational motion during the time course of the simulation. This finding reflects again the sensitivity of the results on the initial starting structure of the peptide prior to the insertion into a bilayer and consecutive hydration (see e.g. [58]). As a conclusion: it is likely that tryptophans may occlude the pore by forming a stable assembly.

At the present stage the results of the simulations suggest a stable 'open-like' structure having all the serines facing the pore. W-in and W^X-in seem to represent a 'closed-like' structure. A gating mechanism can be imagined by a screw-like motion of at least one or two segments. Such rotation (screw-like motion) of one helical TM segment is also proposed for voltage gated Na^+-channels [59–61]. In the light of our data one might assume that the difference between open and closed is controlled by conformational changes in the TM peptide assembly rather than by movement of a single TM segment from or to a pre-existing bundle. More sensitive experiments with respect to the tryptophans are essential to assess a greater conformational space before a mechanism based on computational results can be outlined.

We are aware of the discrepancy between the tilt angle of the TM helix in lipids derived from FTIR spectroscopy ($6.5 \pm 1.7°$) and the tilt angles of the segments obtained after 1 ns simulation (approx. 15°). The FTIR data were collected with lipids in the gel phase; however, the simulation was run under conditions which correspond to a fluid phase of the lipids. It may be possible that the gel phase of the lipids induces a straightening of the helices.

5. Conclusion

We have tested a limited number of Vpu bundles with respect to the orientation of the tryptophans and serines within the TM segment. The current sampling suggests an 'open-like' and 'closed-like' structure in dependence of the positions of the tryptophans. The simulations are sensitive to the initial starting structure, suggesting the need of either more extensive computational sampling of conformational space for a de novo design of the model or further experimentally derived structural constraints including also the extramembranous parts of Vpu.

Acknowledgements

This work was supported with a grant to M.S.P.S. from the Wellcome Trust. F.S.C. thanks the Deutsche Volk Stiftung for a stipend. This work was supported by the EC with a TMR-Research Fellowship for W.B.F. We acknowledge the Oxford Super Computer facility for providing us with computer time.

References

[1] E.A. Cohen, E.F. Terwilliger, J.G. Sodroski, W.A. Haseltine, Nature 334 (1988) 532–534.
[2] K. Strebel, T. Klimkait, M.A. Martin, Science 241 (1988) 1221–1223.
[3] F. Maldarelli, M.Y. Chen, R.L. Willey, K. Strebel, J. Virol. 67 (1993) 5056–5061.
[4] K. Strebel, T. Klimkait, F. Maldarelli, M.A. Martin, J. Virol. 63 (1989) 3784–3791.
[5] U. Schubert, K.A. Clouse, K. Strebel, J. Virol. 69 (1995) 7699–7711.
[6] M. Paul, S. Mazumder, N. Raja, M.A. Jabbar, J. Virol. 72 (1998) 1270–1279.
[7] R.L. Willey, F. Maldarelli, M.A. Martin, K. Strebel, J. Virol. 66 (1992) 7193–7200.
[8] U. Schubert, K. Strebel, J. Virol. 68 (1994) 2260–2271.
[9] U. Schubert, S. Bour, A.V. Ferrer-Montiel, M. Montal, F. Maldarelli, K. Strebel, J. Virol. 70 (1996) 809–819.

[10] S. Bour, U. Schubert, K. Strebel, J. Virol. 69 (1995) 1510–1520.
[11] G.D. Ewart, T. Sutherland, P.W. Gage, G.B. Cox, J. Virol. 70 (1996) 7108–7115.
[12] U. Schubert, A.V. Ferrier-Montiel, M. Oblatt-Montal, P. Henklein, K. Strebel, M. Montal, FEBS Lett. 398 (1996) 12.
[13] F.M. Marassi, C. Ma, H. Gratkowski, S.K. Straus, K. Strebel, M. OblattMontal, M. Montal, S.J. Opella, Proc. Natl. Acad. Sci. USA 96 (1999) 14336–14341.
[14] F.A. Kovacs, T.A. Cross, Biophys. J. 73 (1997) 2511–2517.
[15] F.A. Kovacs, Z. Song, J. Wang, T.A. Cross, Biophys. J. 76 (1999) A126.
[16] V. Wray, R. Kinder, T. Federau, P. Henklein, B. Bechinger, U. Schubert, Biochemistry 38 (1999) 5272–5282.
[17] B. Bechinger, R. Kinder, M. Helmle, T.C.B. Vogt, U. Harzer, S. Schinzel, Biopolymers 51 (1999) 174–190.
[18] W.B. Fischer, M. Pitkeathly, B.A. Wallace, L.R. Forrest, G.R. Smith, M.S.P. Sansom, Biochemistry (2001) in press.
[19] A. Kukol, I.A. Arkin, Biophys. J. 77 (1999) 1594–1601.
[20] A. Kukol, I.T. Arkin, J. Biol. Chem. 275 (2000) 4225–4229.
[21] W.B. Fischer, L.R. Forrest, G.R. Smith, M.S.P. Sansom, Biopolymers 53 (2000) 529–538.
[22] B. Bechinger, R. Kinder, M. Helmle, T.C.B. Vogt, U. Harzer, S. Schinzel, Biopolymers 51 (1999) 174–190.
[23] A.L. Grice, I.D. Kerr, M.S.P. Sansom, FEBS Lett. 405 (1997) 299–304.
[24] P.B. Moore, Q. Zhong, T. Husslein, M.L. Klein, FEBS Lett. 431 (1998) 143–148.
[25] M. Nilges, A.T. Brünger, Protein Eng. 4 (1991) 649–659.
[26] I.D. Kerr, R. Sankararamakrishnan, O.S. Smart, M.S.P. Sansom, Biophys. J. 67 (1994) 1501–1515.
[27] P.D. Adams, I.T. Arkin, D.E. Engelman, A.T. Brunger, Struct. Biol. 2 (1995) 154–162.
[28] A.T. Brünger, X-PLOR Version 3.1. A System for X-ray Crystallography and NMR, Yale University Press, New Haven, CT, 1992.
[29] R.J. Leonard, C.G. Labarca, P. Charnet, N. Davidson, H.A. Lester, Science 242 (1988) 1578–1581.
[30] P. Charnet, C. Labarca, R.J. Leonard, N.J. Vogelaar, L. Czyzyk, A. Gouin, N. Davidson, H.A. Lester, Neuron 2 (1990) 87–95.
[31] A. Villarroel, S. Herlitze, M. Koenen, B. Sakmann, Proc. R. Soc. London Biol. Sci. 243 (1991) 69–74.
[32] K. Imoto, T. Konno, J. Nakai, F. Wang, M. Mishina, S. Numa, FEBS 289 (1991) 193–200.
[33] D. Forst, W. Welte, T. Wacker, K. Diederichs, Nat. Struct. Biol. 5 (1998) 37–46.
[34] E. PebayPeyroula, G. Rummel, J.P. Rosenbusch, E.M. Landau, Science 277 (1997) 1676–1681.
[35] H.J.C. Berendsen, J.R. Grigera, T.P. Straatsma, J. Phys. Chem. 91 (1987) 6269–6271.
[36] W. Kabsch, C. Sander, Biopolymers 22 (1983) 2577–2637.
[37] L. Stella, S. Melchionna, J. Chem. Phys. 109 (1998) 10115–10117.
[38] A. Grice, I.D. Kerr, M.S.P. Sansom, FEBS Lett. 405 (1997) 299–304.
[39] L.R. Forrest, D.P. Tieleman, M.S.P. Sansom, Biophys. J. 76 (1999) 1886–1896.
[40] T.J. Stevens, I.T. Arkin, Protein Struct. Funct. Genet. 36 (1999) 135–143.
[41] G.H.W.M. Meulendijks, T. Sonderkamp, J.E. Dubois, R.J. Nielen, J.A. Kremers, H.M. Buck, Biochim. Biophys. Acta 979 (1989) 321–330.
[42] A.M. O'Connell, R.E. Koeppe II, O.S. Andersen, Science 250 (1990) 1256–1259.
[43] N.D. Lazo, W. Hu, T.A. Cross, J. Chem. Soc. Chem. Commun. (1992) 1529–1531.
[44] W. Hu, N.D. Lazo, T.A. Cross, Biochemistry 34 (1995) 14138–14146.
[45] M.S. Weiss, U. Abele, J. Weckesser, W. Welte, E. Schiltz, G.E. Schulz, Science 254 (1991) 1627–1630.
[46] E. Pebay-Peyroula, G. Rummerl, J.P. Rosenbusch, E.M. Landau, Science 277 (1997) 1676–1681.
[47] M. Hatanaka, R. Kashima, H. Kandori, N. Friedman, M. Sheves, R. Needleman, J.K. Lanyi, A. Maeda, Biochemistry 36 (1997) 5493–5498.
[48] H. Luecke, B. Schobert, H.-T. Richter, C.J.-P., J.K. Lanyi, J. Mol. Biol. 291 (1999) 899–911.
[49] M.S.P. Sansom, I.D. Kerr, G.R. Smith, H.S. Son, Virology 233 (1997) 163–173.
[50] Q. Zhong, T. Husslein, P.B. Moore, D.M. Newns, P. Pattnaik, M.L. Klein, FEBS Lett. 434 (1998) 265–271.
[51] Q. Zhong, D.M. Newns, P. Pattnaik, J.D. Lear, M.L. Klein, FEBS Lett. 473 (2000) 195–198.
[52] L.R. Forrest, A. Kukol, I.T. Arkin, D.P. Tieleman, M.S.P. Sansom, Biophys. J. 78 (2000) 55–69.
[53] F.A. Kovacs, T.A. Cross, Biophys. J. 73 (1997) 2511–2517.
[54] F.A. Kovacs, J.K. Denny, Z. Song, J.R. Quine, T.A. Cross, J. Mol. Biol. 295 (2000) 117–125.
[55] V. Wray, R. Kinder, T. Federau, P. Henklein, B. Bechinger, U. Schubert, Biochemistry 38 (1999) 5272–5282.
[56] F.M. Marassi, C. Ma, H. Gratkowski, S.K. Straus, K. Strebel, O.-M.M., M. Montal, S.J. Opella, Proc. Natl. Acad. Sci. USA 96 (1999) 14336–14341.
[57] P. Henklein, R. Kinder, U. Schubert, B. Bechinger, FEBS Lett. 482 (2000) 220–224.
[58] L.R. Forrest, D.P. Tieleman, M.S.P. Sansom, Biophys. J. 76 (1999) 1886–1896.
[59] C.M. Armstrong, Physiol. Rev. 61 (1981) 644–683.
[60] H.R. Guy, P. Seetharamulu, Proc. Natl. Acad. Sci. USA 83 (1986) 508–512.
[61] C. Armstrong, Physiol. Rev. 72 (1992) S5–S13.